Supplementary Material to "External Prior Guided Internal Prior Learning for Real Noisy Image Denoising"

Anonymous CVPR submission

Paper ID 1047

In this supplementary material, we provide:

1. The closed-form solution of the proposed weighted sparse coding model in the main paper.
2. More denoising results on the real noisy images (with no "ground truth") provided in the dataset [1].
3. More denoising results on the 15 cropped real noisy images (with "ground truth") used in the dataset [2].
4. More denoising results on the 60 cropped real noisy images (with "ground truth") from [2].

1. Closed-Form Solution of the Weighted Sparse Coding Problem (4)

The weighted sparse coding problem in the main paper is:

$$\min_{\boldsymbol{\alpha}} \|\mathbf{y} - \mathbf{D}\boldsymbol{\alpha}\|_2^2 + \|\mathbf{w}^T\boldsymbol{\alpha}\|_1. \tag{1}$$

Since $\mathbf{D}$ is an orthonormal matrix, problem (1) is equivalent to

$$\min_{\boldsymbol{\alpha}} \|\mathbf{D}^T\mathbf{y} - \boldsymbol{\alpha}\|_2^2 + \|\mathbf{w}^T\boldsymbol{\alpha}\|_1. \tag{2}$$

For simplicity, we denote $\mathbf{z} = \mathbf{D^T y}$. Since $\mathbf{w}_i = c * 2\sqrt{2}\sigma^2/(\boldsymbol{\Lambda}_i + \varepsilon)$ is positive (please refer to Eq. (18) in the main paper), problem (2) can be written as

$$\min_{\boldsymbol{\alpha}} \sum_{i=1}^{p^2} ((\mathbf{z}_i - \boldsymbol{\alpha}_i)^2 + \mathbf{w}_i|\boldsymbol{\alpha}_i|). \tag{3}$$

The problem (3) is separable w.r.t. $\boldsymbol{\alpha}_i$ and can be simplified to p^2 scalar minimization problems

$$\min_{\boldsymbol{\alpha}_i} (\mathbf{z}_i - \boldsymbol{\alpha}_i)^2 + \mathbf{w}_i|\boldsymbol{\alpha}_i|, \tag{4}$$

where $i = 1, ..., p^2$. Taking derivative of $\boldsymbol{\alpha}_i$ in problem (4) and setting the derivative to be zero. There are two cases for the solution.

(a) If $\boldsymbol{\alpha}_i \geq 0$, we have

$$2(\boldsymbol{\alpha}_i - \mathbf{z}_i) + \mathbf{w}_i = 0. \tag{5}$$

The solution is

$$\hat{\boldsymbol{\alpha}}_i = \mathbf{z}_i - \frac{\mathbf{w}_i}{2} \geq 0. \tag{6}$$

So $\mathbf{z}_i \geq \frac{\mathbf{w}_i}{2} > 0$, and the solution $\hat{\boldsymbol{\alpha}}_i$ can be written as

$$\hat{\boldsymbol{\alpha}}_i = \text{sgn}(\mathbf{z}_i) * (|\mathbf{z}_i| - \frac{\mathbf{w}_i}{2}), \tag{7}$$

where sgn($\bullet$) is the sign function.

(b) If $\boldsymbol{\alpha}_i < 0$, we have

$$2(\boldsymbol{\alpha}_i - \mathbf{z}_i) - \mathbf{w}_i = 0. \tag{8}$$

The solution is

$$\hat{\boldsymbol{\alpha}}_i = \mathbf{z}_i + \frac{\mathbf{w}_i}{2} < 0. \tag{9}$$

So $\mathbf{z}_i < -\frac{\mathbf{w}_i}{2} < 0$, and the solution $\hat{\boldsymbol{\alpha}}_i$ can be written as

$$\hat{\boldsymbol{\alpha}}_i = \text{sgn}(\mathbf{z}_i) * (-\mathbf{z}_i - \frac{\mathbf{w}_i}{2}) = \text{sgn}(\mathbf{z}_i) * (|\mathbf{z}_i| - \frac{\mathbf{w}_i}{2}). \tag{10}$$

In summary, we have the final solution of the weighted sparse coding problem (1) as

$$\hat{\boldsymbol{\alpha}} = \text{sgn}(\mathbf{D}^{\mathbf{T}}\mathbf{y}) \odot \max(|\mathbf{D}^{\mathbf{T}}\mathbf{y}| - \mathbf{w}/2, 0), \tag{11}$$

where $\odot$ means element-wise multiplication and $|\mathbf{D}^{\mathbf{T}}\mathbf{y}|$ is the absolute value of each entry of the vector $\mathbf{D}^{\mathbf{T}}\mathbf{y}$.

2. More Results on Real Noisy Images in [1]

In this section, we give more visual comparisons of the competing methods on the real noisy images provided in [1]. The real noisy images in this dataset [1] have no "ground truth" images and hence we only compare the visual quality of the denoised images by different methods. As can be seen from Figures 1-4, our proposed method perfomrs better than the state-of-the-art denoising methods. This validates the effectiveness of our proposed external prior guided internal prior learning framework for real noisy image denoising.

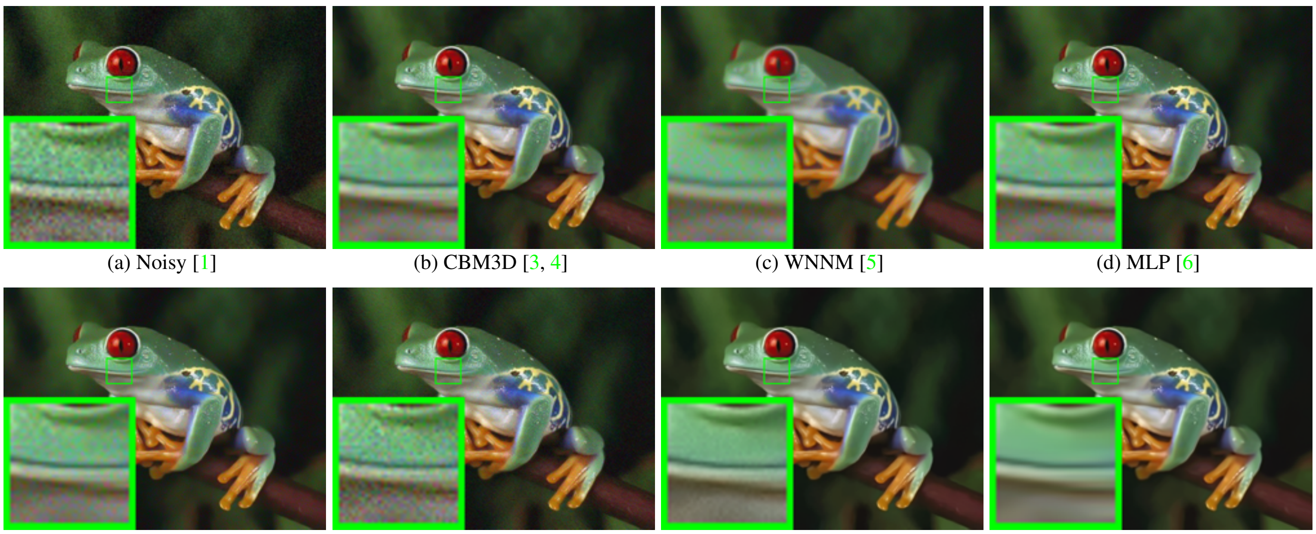

(a) Noisy [1] (b) CBM3D [3, 4] (c) WNNM [5] (d) MLP [6]

(e) TNRD [7] (f) NI [8] (g) NC [1, 9] (h) Ours

Figure 1. Denoised images of the real noisy image "Frog" [1] by different methods. The images are better to be zoomed in on screen.

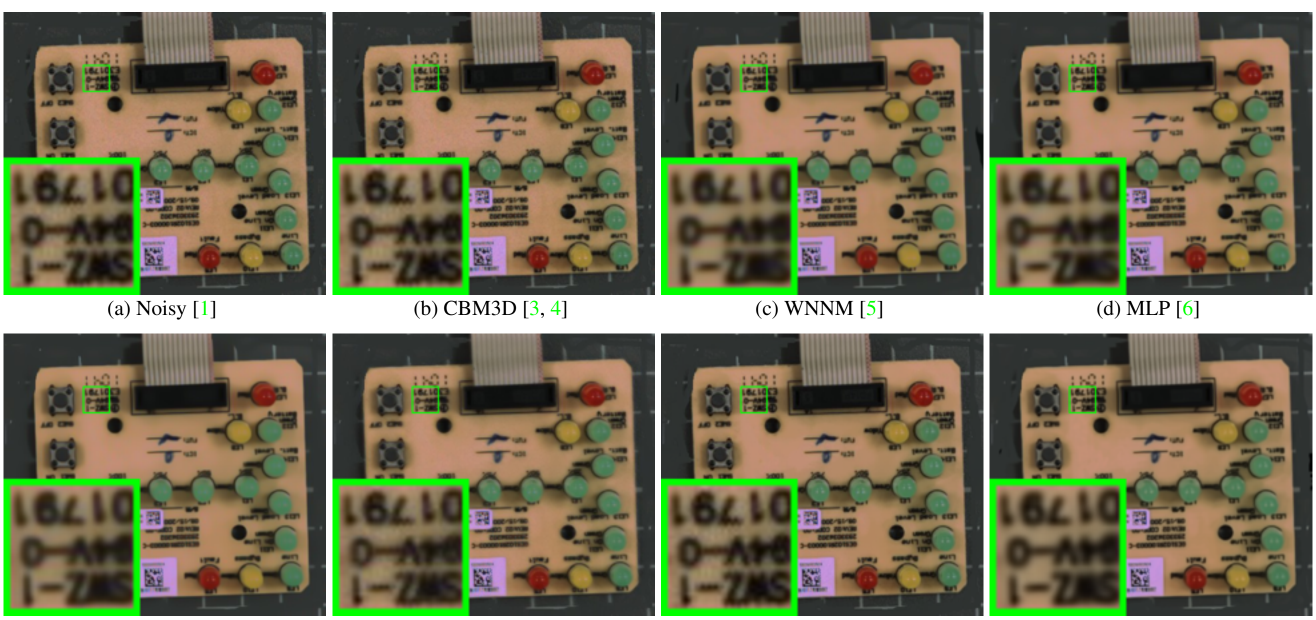

(a) Noisy [1] (b) CBM3D [3, 4] (c) WNNM [5] (d) MLP [6]

(e) TNRD [7] (f) NI [8] (g) NC [1, 9] (h) Ours

Figure 2. Denoised images of the real noisy image "Circuit" [1] by different methods. The images are better to be zoomed in on screen.

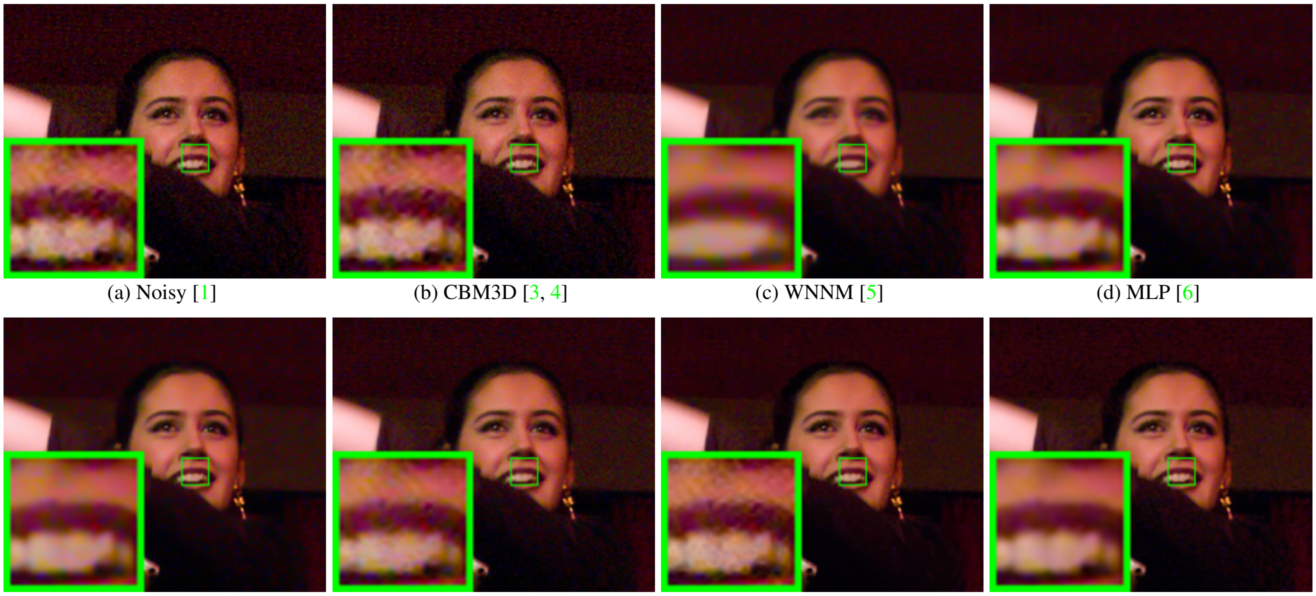

(a) Noisy [1] (b) CBM3D [3, 4] (c) WNNM [5] (d) MLP [6]

(e) TNRD [7] (f) NI [8] (g) NC [1, 9] (h) Ours

Figure 3. Denoised images of the real noisy image "Woman" [1] by different methods. The images are better to be zoomed in on screen.

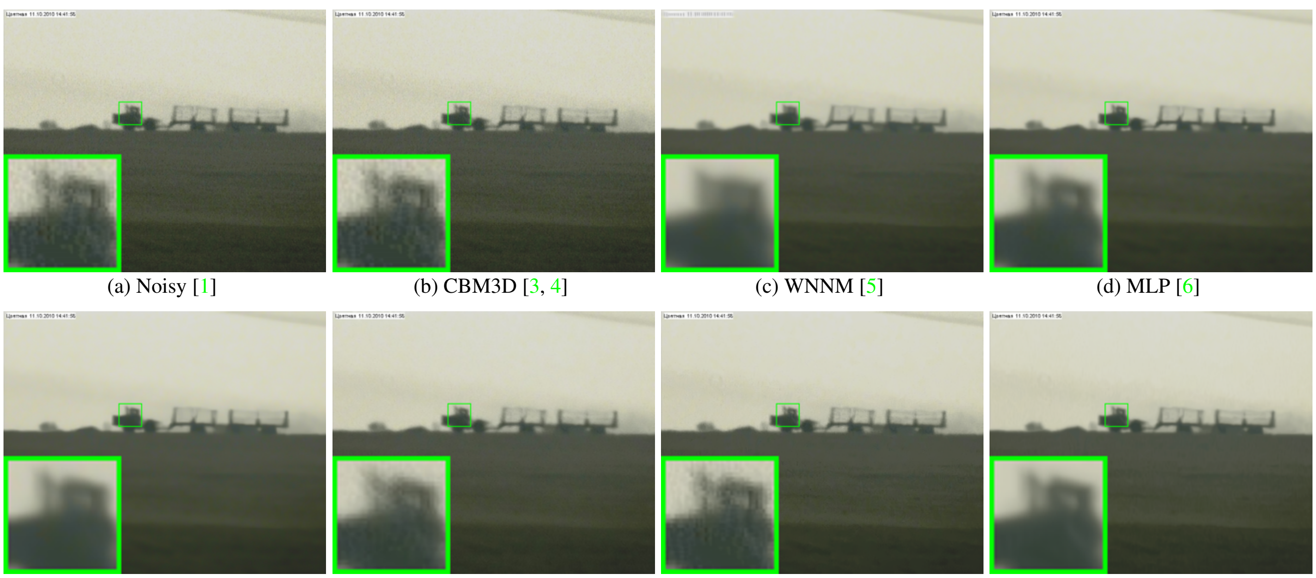

(a) Noisy [1] (b) CBM3D [3, 4] (c) WNNM [5] (d) MLP [6]

(e) TNRD [7] (f) NI [8] (g) NC [1, 9] (h) Ours

Figure 4. Denoised images of the real noisy image "Vehicle" [1] by different methods. The images are better to be zoomed in on screen.

3. More Results on the 15 Cropped Images in [2]

In this section, we provide more visual comparisons of the proposed method with the state-of-the-art denoising methods on the 15 cropped real noisy images used in [2]. As can be seen from Fiures 5-**??**, our proposed method achieves better performance than the the competing methods. This validates the effectiveness of our proposed external prior guided internal prior learning framework for real noisy image denoising.

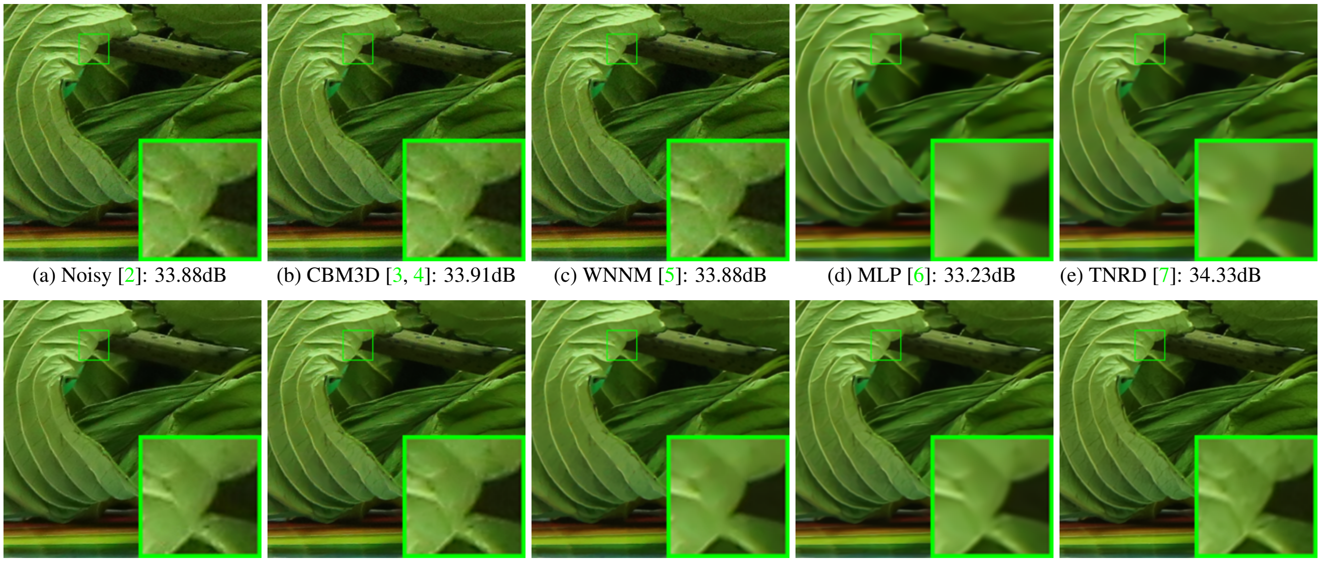

(a) Noisy [2]: 33.88dB (b) CBM3D [3, 4]: 33.91dB (c) WNNM [5]: 33.88dB (d) MLP [6]: 33.23dB (e) TNRD [7]: 34.33dB

(f) NI [8]: 34.87dB (g) NC [9, 1]: 35.69dB (h) CC [2]: 35.37dB (i) Ours: **37.05**dB (j) Mean Image [2]

Figure 5. Denoised images of a region cropped from the real noisy image "Canon 5D Mark 3 ISO 3200 2" [2] by different methods. The images are better to be zoomed in on screen.

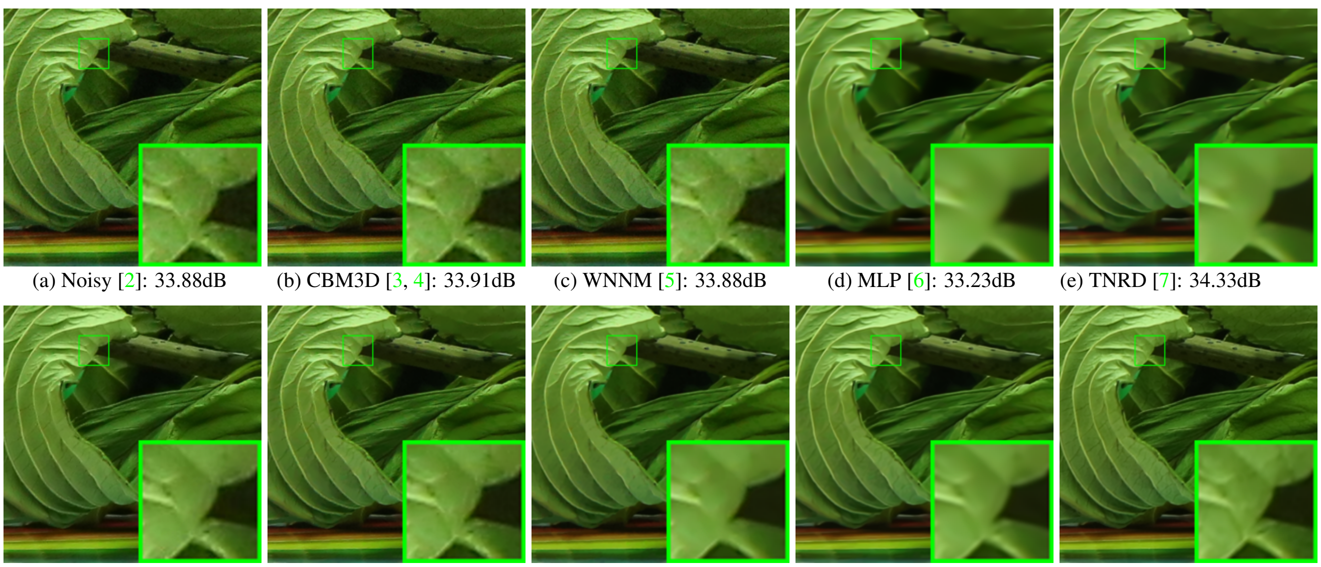

(a) Noisy [2]: 33.88dB (b) CBM3D [3, 4]: 33.91dB (c) WNNM [5]: 33.88dB (d) MLP [6]: 33.23dB (e) TNRD [7]: 34.33dB

(f) NI [8]: 34.87dB (g) NC [9, 1]: 35.69dB (h) CC [2]: 35.37dB (i) Ours: **37.05**dB (j) Mean Image [2]

Figure 6. Denoised images of a region cropped from the real noisy image "Canon 5D Mark 3 ISO 3200 2" [2] by different methods. The images are better to be zoomed in on screen.

References

[1] M. Lebrun, M. Colom, and J. M. Morel. The noise clinic: a blind image denoising algorithm. `http://www.ipol.im/pub/art/2015/125/`. Accessed 01 28, 2015. 1, 2, 3, 4

[2] S. Nam, Y. Hwang, Y. Matsushita, and S. J. Kim. A holistic approach to cross-channel image noise modeling and its application to image denoising. *IEEE Conference on Computer Vision and Pattern Recognition (CVPR)*, pages 1683–1691, 2016. 1, 3, 4

[3] K. Dabov, A. Foi, V. Katkovnik, and K. Egiazarian. Image denoising by sparse 3-D transform-domain collaborative filtering. *IEEE Transactions on Image Processing*, 16(8):2080–2095, 2007. 2, 3, 4

[4] K. Dabov, A. Foi, V. Katkovnik, and K. Egiazarian. Color image denoising via sparse 3D collaborative filtering with grouping constraint in luminance-chrominance space. *IEEE International Conference on Image Processing (ICIP)*, pages 313–316, 2007. 2, 3, 4

[5] S. Gu, L. Zhang, W. Zuo, and X. Feng. Weighted nuclear norm minimization with application to image denoising. *IEEE Conference on Computer Vision and Pattern Recognition (CVPR)*, pages 2862–2869, 2014. 2, 3, 4

[6] H. C. Burger, C. J. Schuler, and S. Harmeling. Image denoising: Can plain neural networks compete with BM3D? *IEEE Conference on Computer Vision and Pattern Recognition (CVPR)*, pages 2392–2399, 2012. 2, 3, 4

[7] Y. Chen, W. Yu, and T. Pock. On learning optimized reaction diffusion processes for effective image restoration. *IEEE Conference on Computer Vision and Pattern Recognition (CVPR)*, pages 5261–5269, 2015. 2, 3, 4

[8] Neatlab ABSoft. Neat Image. https://ni.neatvideo.com/home. 2, 3, 4

[9] M. Lebrun, M. Colom, and J.-M. Morel. Multiscale image blind denoising. *IEEE Transactions on Image Processing*, 24(10):3149–3161, 2015. 2, 3, 4